



Virtual screening and synthesis of quinazolines as novel JAK2 inhibitors

Su Hui Yang^a, Daulat Bikram Khadka^a, Suk Hee Cho^a, Hye-Kyung Ju^{b,c}, Kwang Youl Lee^a, Ho Jae Han^d, Kyung-Tae Lee^{b,c}, Won-Jea Cho^{a,*}

^a College of Pharmacy and Research Institute of Drug Development, Chonnam National University, Gwangju 500-757, Republic of Korea

^b Department of Biomedical Science, College of Medical Science, Kyung-Hee University, Seoul 130-701, Republic of Korea

^c Department of Pharmaceutical Biochemistry, College of Pharmacy, Kyung-Hee University, Seoul 130-701, Republic of Korea

^d Department of Veterinary Physiology, College of Veterinary Medicine, Chonnam National University, Gwangju 500-757, Republic of Korea

ARTICLE INFO

Article history:

Received 15 September 2010

Revised 23 November 2010

Accepted 23 November 2010

Available online 30 November 2010

Keywords:

JAK2
Quinazolines
Virtual screening
SurflexDock
Apoptosis
Stem cell
AG490

ABSTRACT

JAK2 is an important target in multiple processes associated with tumor growth. In this study, virtual screening was employed for hit compound identification with chemical libraries using SurflexDock. Subsequently, hit optimization for potent and selective candidate JAK2 inhibitors was performed through synthesis of diverse C-1 substituted quinazoline derivatives. A novel compound **5p**, (6,7-dimethoxyquinazolin-4-yl)naphthalen-1-ylamine, was thus obtained. JAK2 inhibitory activity of **5p** was 43% at 20 μ M and this was comparable to AG490, a representative JAK2 inhibitor. Moreover, **5p** showed a positive correlation between JAK2 inhibition and cytotoxicity; **5p** treatment in HT-29 cells strongly inhibited JAK2 activation and subsequent STAT3 phosphorylation, reduced anti-apoptotic protein levels, and finally induced apoptosis. This suggests that compound **5p** is a candidate inhibitor of JAK2 and its downstream STAT3 signaling pathway for antitumor therapy. In the docking model, the quinazoline template of **5k**, the lead compound, occupied a hydrophobic region such as Leu856, Leu855, Ala880, Leu932 and Gly935, and the highly conserved hydrogen bond was created by 6-OMe of the ring template, which binds to the NH of Arg980. Moreover, hydrophobic interactions were identified between morpholine moiety and the hydrophobic region formed by Leu855, Ala880, Tyr931, Val911 and Met929. Also, compound **5k** more strongly inhibited JAK2 phosphorylation in mouse embryonic stem cells than AG490. Our study shows the successful application of virtual screening for lead discovery and we propose that the novel compound **5p** can be an effective JAK2 inhibitor candidate for further antitumor agent research.

© 2010 Elsevier Ltd. All rights reserved.

1. Introduction

JAK2 is a member of the Janus kinases (JAKs), which are intracellular non-receptor protein tyrosine kinases including Jak1, Jak2, Jak3, and Tyk2. Each kinase has seven Janus homology domains: a typical kinase domain (JH1) close to the C-terminus, a pseudokinase domain (JH2) that is nearly identical to JH1 in amino acid sequence, and the remaining homology regions (JH3–JH7) containing the FERM domain, which regulates binding to cytokine receptors.¹ JAK2 associates with various cytokine receptors; it is responsible for signal transduction by mediating tyrosine phosphorylation.² The cellular responses to cytokines are essential for normal cell development and function. In other words, if the kinase activity is not properly regulated, there can be detrimental effects such as abnormal cell proliferation.

Jak2 kinase activity is controlled mainly by the inhibitory effect of the JH2 domain against the activation of the JH1 domain.^{2b,3} In

the probable mechanism, cytokine binds to the corresponding cell-surface receptor to which JAK2 tyrosine kinase attaches. The JH1 domain of JAK2 contains typical tyrosines (e.g., Y1007/Y1008) and autophosphorylates the dual tyrosines, leading to a conformational change in the receptor for JAK2 activation.⁴ When the phosphorylation occurs, the suppressive function of JH2 is relieved.⁵ The activated JAK2 phosphorylates specific tyrosine and serine residues of the receptor, creating docking sites for the signal transducers and activators of transcription (STATs). Then, STATs bind the receptor, allowing JAK2 in turn to phosphorylate STATs. Finally, phosphorylated STATs are dissociated from the receptor, form dimers, and translocate into the nucleus, where gene transcription is regulated.

The role of the JH2 domain of JAK2 in controlling kinase activity is worth noting due to the pathological consequences of mutations in this domain. In 1995, the possibility of de-regulation of JAK2 activity was first suggested through a single mutation in the JH2 domain.⁶ Later, quite surprisingly, five independent research groups simultaneously reported the presence of the JAK2 V617F mutation in several myeloproliferative diseases; it was detected in most polycythemia vera patients and in half of essential

* Corresponding author. Fax: +82 62 530 2911.

E-mail address: wjcho@jnu.ac.kr (W.-J. Cho).

thrombocytopenia patients.⁷ This mutation was somatically acquired and was limited to the myeloid lineages, implying that the mutation was present and maintained in a myeloid lineage progenitor stem cell. In addition, chromosomal translocation of JAK2 or other JAK2 somatic mutations such as amino acid substitutions and deletions are characterized in various leukemias.⁸ Therefore, the development of a potent, selective JAK2 inhibitor seems quite promising for anticancer therapy.

As the first JAK2 inhibitor, AG490 was identified through high-throughput screening in 1995.⁹ It is a member of the tyrphostin family of tyrosine kinase inhibitors, and it efficiently blocks the growth of leukemic cells by inducing cellular apoptosis. However, AG490 lacks specificity for JAK2 so that the induced apoptosis in cancer cells treated with AG490 may not result from JAK2 inhibition. Additionally, subsequent reports revealed that AG490 inhibits JAK2/STAT3 signaling in vitro, but only at high concentrations (IC_{50} = 50–100 μ M), which translates into limited activity in vivo.^{9,10} This has led to a search for a selective JAK2 inhibitor but there is no effective inhibitor of JAK2 that is currently available for clinical use.

Recently, several X-ray structures of JAK2 in complexes with a number of small molecule inhibitors, including quinoxaline,¹¹ azaindole,¹² and 2-aminopyrazolo[1,5-a]pyrimidine¹³ as shown in Figure 1, have been determined.

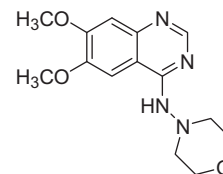
Virtual screening has been considered an important in silico technique for finding novel compounds and has led to many successes in drug development. Structure-based virtual screening methods are emerging as reliable and complementary approaches through the determination of the X-ray crystal structures of ligand–protein complexes.

In this study, we describe the virtual screening of molecules to recognize potential hits for JAK2 inhibitors using a SurflexDock program. Novel potential leads were selected as identified molecules using consensus docking score, and these compounds were evaluated for JAK2 inhibitory activities. Through virtual screening, the lead compound (6,7-dimethoxy-quinazolin-4-yl)-morpholin-4-yl-amine (**5k**) was found as shown in Figure 2. Next, we tried to optimize the lead compound (**5k**) through chemical modification of quinazoline by introducing various amines on the C-1 position. The synthesized quinazoline analogs were utilized to evaluate their effects on JAK2 inhibition and cytotoxicity against three cancer cell lines. In addition, we investigated the effects of the potent compound **5p** on the downstream JAK2/STAT3 signaling pathway and the mechanism of compound **5p** to induce apoptosis by flow cytometry.

2. Results and discussion

2.1. Chemistry

In order to improve biological activities or diminish toxicity, or increase absorption lead optimization is operated. For finding out



(6,7-Dimethoxyquinazolin-4-yl)morpholin-4-yl-amine (**5k**)

Figure 2. Structure of hit compound selected from virtual screening.

more potent molecules than lead compound **5k**, we tried to synthesize diverse modified compounds. The quinazoline derivatives were synthesized as illustrated in Scheme 1. The commercially available 2-amino-4,5-dimethoxybenzoic acid **1** was reacted with formamidine acetate to give 6,7-dimethoxy-3*H*-quinazolin-4-one **2** in 89% yield. Treatment of the quinazolinone **2** with thionyl chloride afforded the corresponding imine chloride **3** in 92% yield. The imine chloride **3** was then reacted with various amines in isopropanol or DMF to afford the desired quinazolines **5** in moderate yields.

2.2. Identification of hit by virtual screening

For a virtual screening and a docking study, we used Surflex-Dock in Sybyl version 8.1.1 (Tripos Associates) operating under Red Hat Linux 4.0 on an IBM computer (Intel Pentium 4, 2.8 GHz CPU, 1 GB memory). The structures of the inhibitors were drawn in the Sybyl package with standard bond lengths and angles and minimized using the conjugate gradient method. The Gasteiger–Huckel charge, with a distance-dependent dielectric function, was applied for the minimization process. We chose the 3E63 (PDB code #) structure from the Protein Data Bank, and the structure was polished as follows. The JAK2 protein was analyzed by Structure-Preparation Tool in Sybyl. The angles of seven side chains such as Glu846, Asn859, Gln872, Arg947, Gln1003, Lys1053 and Asp1092 were corrected. After adding hydrogen, the charges loaded on the protein and ligand with AMBER FF99 and Gasteiger–Marsili, respectively. The side chain amides were also fixed and two bumping amino acids such as Ser904 and Tyr972 were adjusted.

We performed flexible docking with SurflexDock on a relatively small library containing 2000 drug-like molecules extracted from commercial and in-house databases. SurflexDock performs the docking through automatic way to the ligand binding pocket using a protocol-based method. The protocol is a critical and essential factor of the docking algorithm and is a computational demonstration of proposed ligands that interact with the binding site. SurflexDock's scoring function uses hydrophobic, polar, repulsive, entropic, and solvation terms. After extracting the aminoindazole ligand which was in active site of 2E63, the protocol was produced.

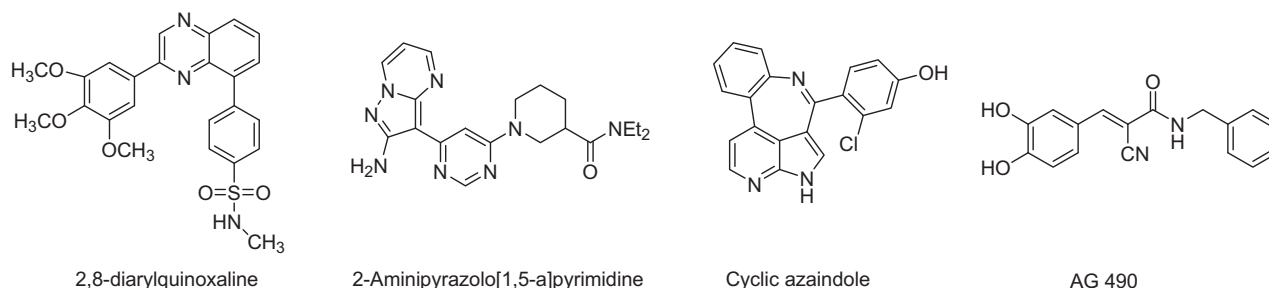
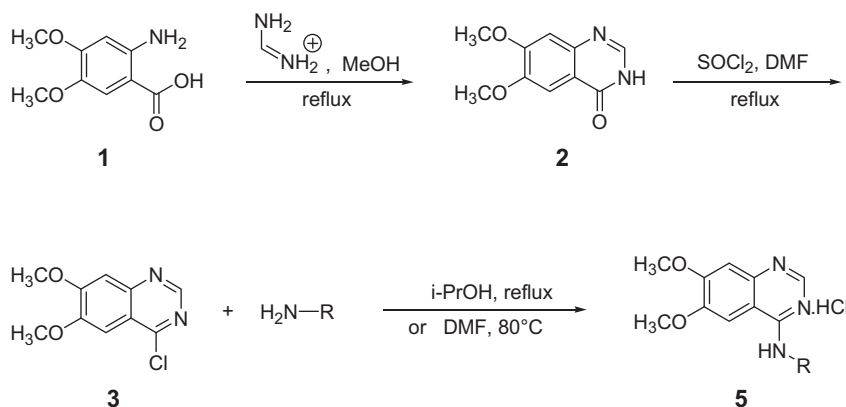


Figure 1. Structures of the inhibitors interacting with ATP-binding site of JAK2.



Scheme 1. Synthesis of quinazolines **5**.

The chemical structures were drawn in Sybyl and saved as mol2 file into database. The SurflexDock was carried out using the above database as ligand source with maximum number of poses per ligand with 20.

Docking calculations of the selected compounds led to the identification of plausible inhibitors producing 12 hits with high scores. The hit compounds were primarily used to test JAK2 inhibition activity. Among the 12 compounds, compound **5k**, a quinazoline derivative, displayed a good docking score (6.25) and the most active potency (44.42% inhibition at 20 μ M). Thus, the virtual screening approach yielded a novel and potent hit compound JAK2 inhibitor from a limited selection of compounds.

The quinazoline template occupied a hydrophobic region such as Leu856, Leu855, Ala880, Leu932, and Gly935. The highly conserved hydrogen bond was created by 6-OMe of the ring template, which binds to the NH of Arg980. Moreover, hydrophobic interactions were identified between the morpholine moiety and the hydrophobic region formed by Leu855, Ala880, Tyr931, Val911, and Met929 as illustrated in Figure 3.

2.3. JAK2 inhibitory activity and cytotoxicity of quinazoline compounds

All synthesized quinazoline compounds were tested for JAK2 inhibition and in vitro cytotoxicity using HTScan® JAK2 Kinase Assay Kit. AG490, a well-known JAK2 inhibitor, was used as a positive control. The JAK2 inhibitory effect was assessed after treatment with 20 μ M of each compound. Most compounds did not have potent JAK2 inhibitory activity, but compounds **5k** and **5p** showed similar JAK2 inhibition (44.42% and 43.03%, respectively) to AG490 (Table 1). Also, the inhibition of JAK2 activity was detected at 10, 20, and 50 μ M of compound **5p** in a dose-dependent manner (Figure 4). In many cases, the enzyme activity does not correlate well with cytotoxicity and this can be explained by different solubility or poor membrane permeability.

Cytotoxicity was determined against three different human tumor cell lines: SK-OV-3 (human ovarian tumor), HeLa (human cervix tumor), and HT-29 (human colon tumor). The IC₅₀ values are displayed in Table 1. While no significant cytotoxic effect was detected with AG490, compound **5p** showed potent cytotoxicity at

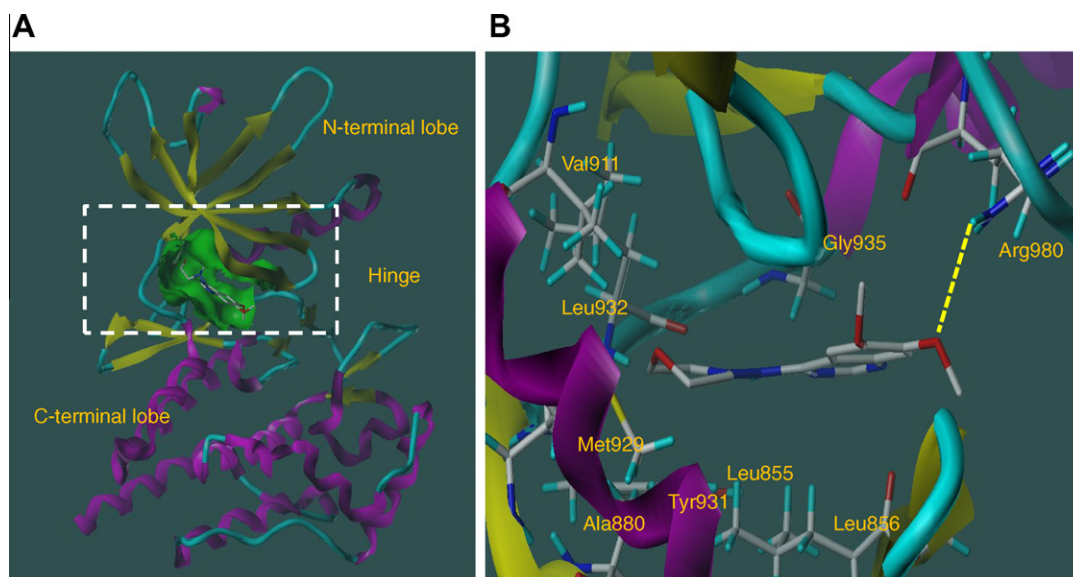
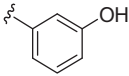
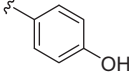
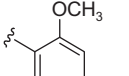
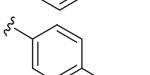
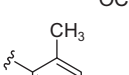
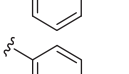
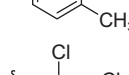
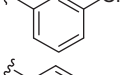
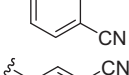
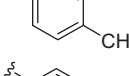
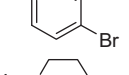
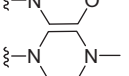
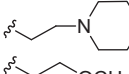
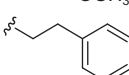
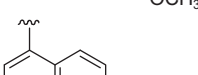
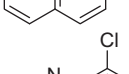
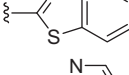
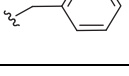


Figure 3. (A) Ribbon diagram illustrating the crystal structure of JAK2 with compound **5k** bound to the active site; (B) graphical representation of the binding mode of compound **5k** to the ATP-binding site of JAK2. For clarity, only the Arg980 residue is displayed, and hydrogen bond interactions are represented by yellow dashed lines.

Table 1
JAK2 inhibitory effect and cytotoxicity of quinazolines **5a–r**

No.	Compound	R	JAK2 inhibitory effect (%)	IC ₅₀ (μM)		
				SK-OV-3	HeLa	HT-29
1	5a		23.799	37.476	43.946	59.718
2	5b		33.126	74.595	51.472	92.994
3	5c		29.418	>100	>100	>100
4	5d		— [‡]	>100	— [‡]	— [‡]
5	5e		10.589	>100	>100	>100
6	5f		18.426	91.901	99.547	57.865
7	5g		— [§]	— [§]	— [§]	— [§]
8	5h		— [§]	— [§]	— [§]	— [§]
9	5i		— [§]	— [§]	— [§]	— [§]
10	5j		29.345	>100	— [‡]	>100
11	5k		44.415	>100	>100	>100
12	5l [†]		— [§]	— [§]	— [§]	— [§]
13	5m		29.457	>100	>100	>100
14	5n		38.036	>100	>100	>100
15	5o		25.297	>100	>100	>100
16	5p		43.025	16.729	8.019	7.650
17	5q		14.444	>100	>100	>100
18	5r [†]		14.475	>100	>100	>100
Reference	AG490		55.081	— [‡]	>100	78.523

[†] Not HCl salt.[‡] No significant effect.[§] Not tested due to solubility problem of the compound.

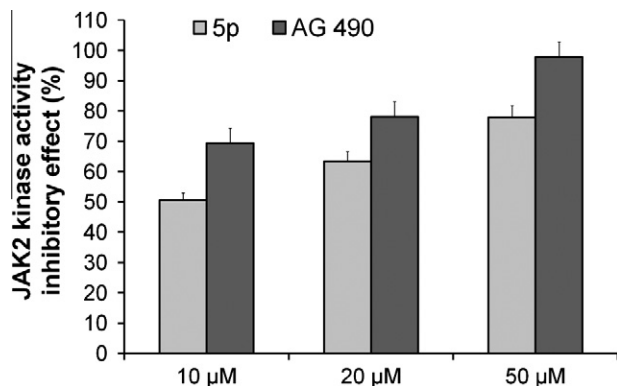


Figure 4. The JAK2 inhibitory effect (%) of **5p** and AG490 at varying concentrations; JAK2 kinase activities were measured using Assay Kit (Cell Signaling Technology) system. Data are the means \pm SD of three independent experiments.

low micromolar concentration. Interestingly, a positive correlation between JAK2 inhibition and cytotoxicity was detected in **5p** treatment but not in **5k** treatment. So, further in vitro screening was carried out using **5p**.

As compound **5k** was identified as the lead compound through the initial screening for JAK2 inhibition by JAK2 Kit (44.42% of JAK2 inhibition), we investigated to see whether **5k** efficiently inhibits phosphorylation of Jak2 protein in mouse embryonic stem cells (ESC) (Figure 5). As a result, the level of phosphorylated JAK2 (p-JAK2) was increased with IL-6 pretreatment, and compound **5k** markedly inhibited the level of p-JAK2 while AG490 reduced the level of p-JAK2 to the basal level.

2.4. Effects of quinazoline **5p** on inhibition of phosphorylation of JAK2 and STAT3

To examine whether JAK2 activity is down-regulated by compound **5p**, the phosphorylation of JAK2 was examined by Western blot analysis in HT-29 cells. As shown in Figure 6A, **5p** treatment significantly attenuated p-JAK2 level dose-dependently (10, 20 μ M). On the other hand, AG490 treatment at the same concentration did not inhibit IL-6 induced phosphorylation of JAK2 protein (data not shown). With fivefold more AG490 (50, 100 μ M), a slight decrease in p-JAK2 protein expression was detected. Moreover, the total protein expression of JAK2 did not

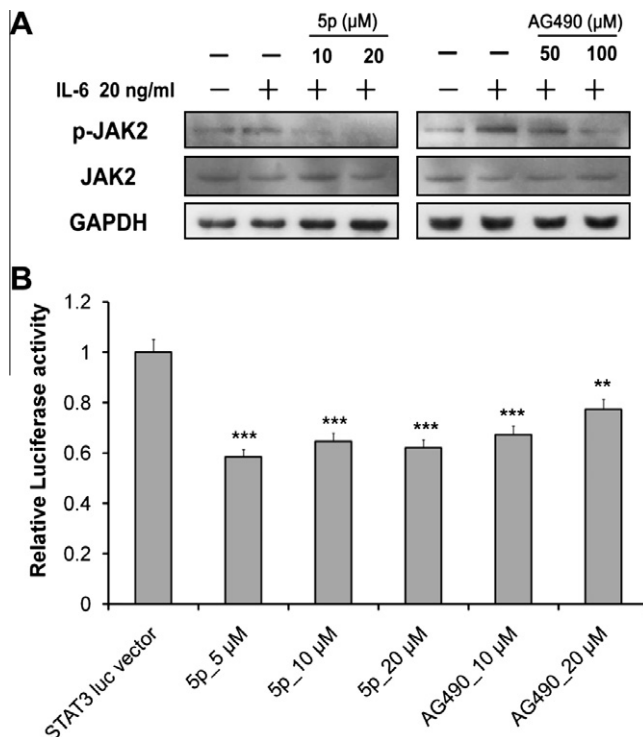


Figure 6. (A) Expression level of JAK2 and p-JAK2 after treatment with **5p** and AG490; HT-29 cells were treated with IL-6 for 0.5 h, then with **5p** (10, 20 μ M) and AG490 (50, 100 μ M). The expressions were examined using Western blotting. GAPDH was used as an internal control. A representative immunoblot of three separate experiments is shown. (B) The inhibitory effect on luciferase activity of STAT3 after treatment with **5p** and AG490 at varying concentrations; HT-29 cells were transfected with the STAT3-dependent luciferase reporter construct pSTAT3-Luc. After treatment with **5p** or AG490 for 1 h in transfected HT-29 cells, the luciferase assay was performed. Data are the means \pm SD of three independent experiments. ** p < 0.01, *** p < 0.001 vs control group; significance was determined using Student's t -test.

change with **5p** treatment, indicating that **5p** inhibits JAK2 activation.

JAKs have been reported to be important for mediating the constitutive STAT activation that has been detected in many human cancer cells.¹⁴ STAT3 is one of the signaling pathways induced by activated JAK2, and it plays an essential role in mitogenic and cell

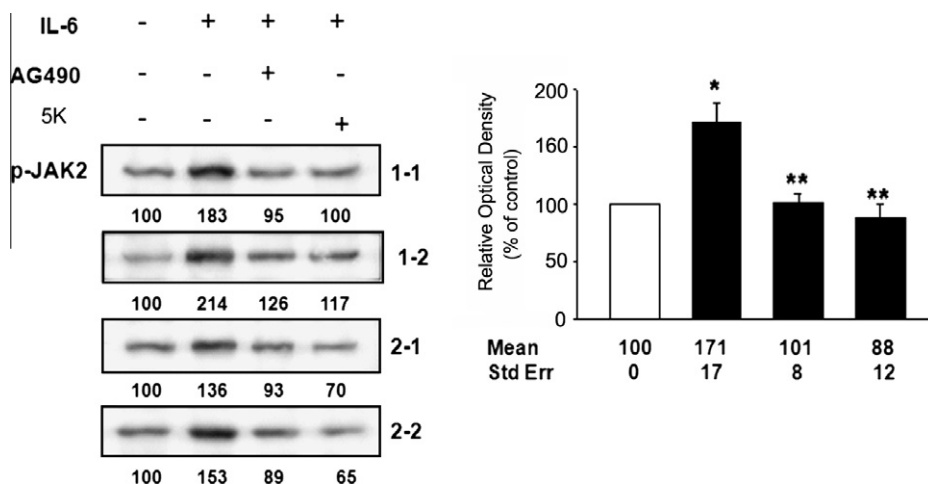


Figure 5. Expression level of p-JAK2 after treatment with **5k** and AG490 in mouse ESC; mouse ESC was treated with IL-6 for 1 h, then with **5k** and AG490 (20 μ M). The expressions were examined using Western blotting. A representative immunoblot is shown. Relative optical density (% of control) is displayed next. Data are the means \pm SD of three independent experiments. * p < 0.1, ** p < 0.01 vs control group; significance was determined using a Student's t -test.

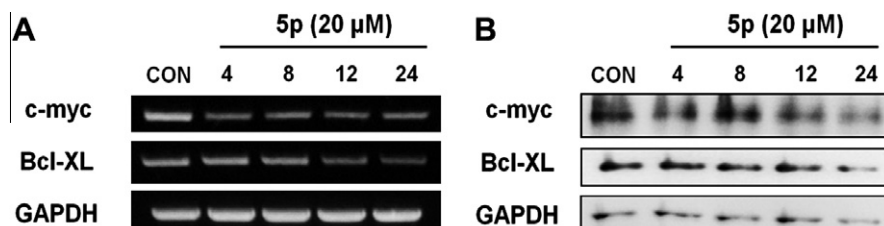


Figure 7. The expression level of c-myc and Bcl-XL with **5p** (20 μM) in HT-29 cells; cells were treated with **5p** (20 μM) for the indicated time, then total RNA and lysates were prepared for RT-PCR (A) and Western blotting (B) of c-myc and Bcl-XL. GAPDH was used as an internal control.

survival.¹⁵ To verify STAT3 regulation by compound **5p**, we measured the transcriptional activity of STAT3 by using pSTAT3-Luc plasmid, which was generated by inserting multidimerized STAT3-specific binding sites upstream of a luciferase reporter gene. Cells were transiently transfected with this plasmid and then stimulated with IL-6 (20 ng/ml) either in the presence or absence of compound **5p**. Pretreatment with **5p** significantly reduced STAT3-dependent luciferase activity, but **5p** and AG490 have not shown dose-dependency (Figure 6B).

Additionally, our results agreed with the previous report that AG490 inhibited JAK2/STAT3 signaling in vitro only at high concentrations.

2.5. Effects of quinazoline **5p** on the expression of c-myc and Bcl-XL

To determine whether this inhibitory effect of **5p** on c-myc and Bcl-XL expression is associated with the induction of apoptosis in HT-29 cells, we quantified the mRNA and protein levels of c-myc and Bcl-XL by RT-PCR and Western blotting, respectively.

The increase in activated STAT3 induces target proteins such as c-myc or Bcl-XL, which are anti-apoptotic.¹⁶ Since these target proteins are involved in the control of apoptosis and cell cycle progression, STAT3 is pathogenetically important by regulating the expression of anti-apoptotic proteins.^{16,17} Based on the data presented here (Figure 7A and B), the expressions of c-myc and Bcl-XL were affected by treatment with 20 μM **5p**, and both levels were decreased in a time-dependent manner. These results suggest that **5p**-mediated suppression of the JAK2/STAT3 pathway was accompanied by down-regulation of c-myc and Bcl-XL, finally resulting in apoptosis. The inhibitory effect of **5p** on the anti-apoptotic proteins caused cytotoxic effect on cells that corresponds to the result of cytotoxicity of **5p** as explained below.

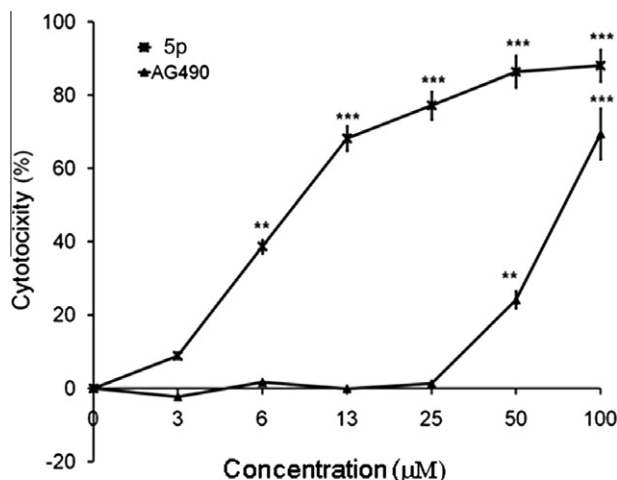


Figure 8. Cytotoxicity (%) of **5p** and AG490 in the HT-29 cell line at varying concentrations.

2.6. Cytotoxicity of quinazoline **5p** and AG490 in HT-29 cell

The cytotoxicity of compound **5p** and AG490 was determined by increasing their concentrations in HT-29 cells (Figure 8). AG490 had no cytotoxicity until it was increased to 25 μM, and about 75 μM was required to inhibit cell growth by 50%. However, the cytotoxicity of **5p** increased in a dose-dependent manner, and about 7 μM **5p** was required for 50% inhibition of cell growth.

2.7. Cell cycle dynamics of quinazoline **5p** by flow cytometry

As compound **5p** had a significant cytotoxic effect on human colon adenocarcinoma HT-29 cells, we further examined the precise effect of **5p** on the cell cycle of HT-29 cells by flow cytometry (Figure 9A). When cells were treated with **5p** (5, 10 and 20 μM) for 24 h, the cell cycle arrest at G2/M phase was significantly increased, accompanying a decrease in G1 phase when compared

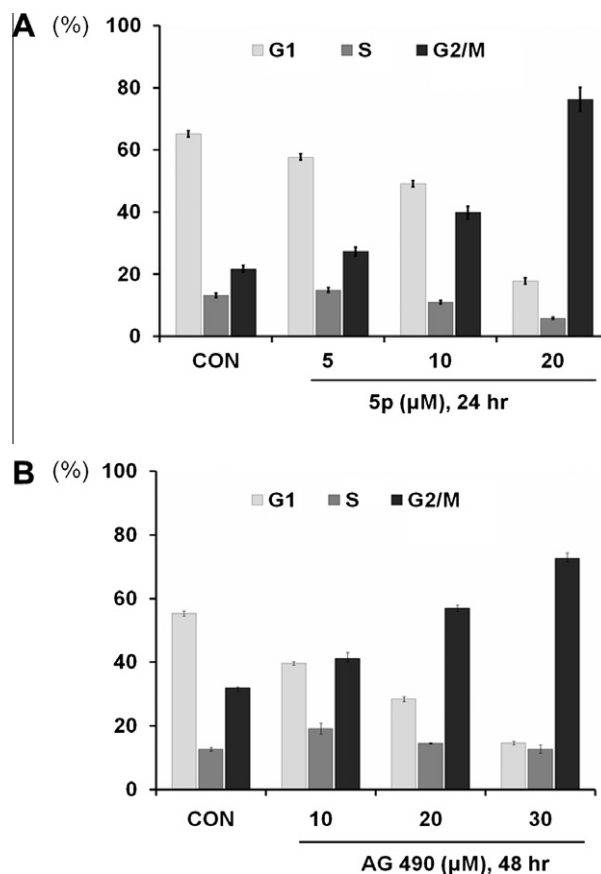


Figure 9. Effects of **5p** and AG490 on cell cycle arrest in HT-29 cells; cells were treated with **5p** (5, 10 and 20 μM) for 24 h (A) or AG490 (10, 20 and 30 μM) for 48 h (B), and then harvested, and fixed in 70% ethanol. After staining with propidium iodide, DNA contents were analyzed by flow cytometry. Data are the means ± SD of three independent experiments. ***p* < 0.01, ****p* < 0.001 vs non-treated control group; significance was determined by the Student's *t*-test.

with the untreated control cells. Moreover, treatment with AG490 (10, 20 and 30 μ M) for 48 h also induced G2/M phase arrest (Figure 9B). These results explained the positive correlation between JAK2 inhibition and cytotoxicity of compound **5p** in HT-29 cells in that **5p** inhibited JAK2/STAT3 signaling, reduced consequent anti-apoptotic protein levels, and finally caused apoptosis by inducing G2/M arrest.

3. Conclusion

A structure-based virtual screening approach was used to identify the compounds that inhibit JAK2 activity. A docking study was applied to find a lead compound in a time- and cost-efficient manner. This approach employed the SurflexDock program in the Sybyl package with an in-house and commercial chemical database. We identified a C-1 morpholine-substituted quinazoline compound as a novel strong inhibitor of JAK2 through virtual screening of 2000 compounds, and 12 compounds were selected for actual testing in a biochemical assay. Among these molecules, one compound suppressed the enzymatic activity of JAK2 with 44% inhibition at 20 μ M, and was used the starting compound as a JAK2 inhibitor. We selected the hit compound **5k** as the lead for the design of new JAK2 inhibitors for further synthetic processes. Substituents at the C-1 position were synthesized for optimization of JAK2 inhibitory activity. In the docking model, the quinazoline template of **5k** occupied hydrophobic regions such as Leu856, Leu855, Ala880, Leu932, and Gly935, and the highly conserved hydrogen bond was created by 6-OMe of the ring template, which binds to the NH of Arg980. Moreover, hydrophobic interactions were identified between the morpholine moiety and the hydrophobic region formed by Leu855, Ala880, Tyr931, Val911, and Met929.

Among the newly synthesized derivatives, compound **5p** showed a positive correlation between JAK2 inhibition and cytotoxicity. **5p** treatment in HT-29 cells strongly inhibited JAK2 activation and the subsequent STAT3 phosphorylation, reduced the anti-apoptotic protein levels, and finally induced apoptosis, probably due to G2/M arrest. We have therefore demonstrated that compound **5p** is a potent and selective inhibitor of the JAK2/STAT3 pathway. Compound **5p** was identified as a candidate for further exploration of the hypothesis that modulation of JAK2/STAT3 signaling pathway could be beneficial in cancer treatment.

4. Experimental

4.1. General remarks

Chemicals were provided by Aldrich Chemical Co. or Tokyo Chemical Industry Co. and utilized without further purification. Solvents were distilled prior to use. Nuclear magnetic resonance (NMR) spectra were taken on Bruker AMX-R300 for ^1H NMR and were calibrated with tetramethylsilane. The NMR data are displayed as follows: chemical shifts (δ) are recorded in ppm, coupling constants (J) in hertz (Hz), integrity in the number of protons, and multiplicity in s (singlet), d (doublet), t (triplet), and m (multiplet). Mass spectra were obtained on Shimadzu LCMS-2010EV utilizing the electron-spray ionization (ESI) method. Thin-layer chromatography (TLC) was carried out using plates coated with Silica Gel 60 F₂₅₄ purchased from Merck. Column chromatography was performed with Merck Silica Gel 60 (70–230 mesh).

4.1.1. 6,7-Dimethoxy-3H-quinazolin-4-one (2)

A solution of 2-amino-4,5-dimethoxybenzoic acid **1** (2.02 g, 10 mmol) and formamidinium acetate (2.10 g, 20 mmol) in 2-methoxyethanol (50 mL) was refluxed overnight. After evaporation of the solvent, the residue was stirred after adding 10% NH_4OH

(18 mL). The resulting residue was filtered, washed with water, and dried to give compound **2** as a dark brown solid (1.83 g, 89%). ^1H NMR (300 MHz, $\text{DMSO}-d_6$) δ : 12.11 (1H, s, NH), 8.0 (1H, s, $-\text{N}=\text{CH}$), 7.44 (1H, s, aromatic-H), 7.14 (1H, s, aromatic-H), 3.90 (3H, s, $-\text{OCH}_3$), 3.87 (3H, s, $-\text{OCH}_3$).

4.1.2. General procedure for the synthesis of quinazolines 5

A mixture of compound **2** (1.82 g, 8.8 mmol) and DMF (30 drops) in SOCl_2 (50 mL) was refluxed for 7 h. The excess SOCl_2 was removed by vacuum distillation. The residue was stirred with diethyl ether, filtered, washed, and dried to give compound **3** as a beige solid (1.83 g, 92%). A mixture of compound **3** and various amines in 2-propanol or DMF was refluxed. Upon completion of the reaction, it was cooled in an ice bath. The residue was filtered, washed, and dried to isolate the product.

4.1.3. 3-(6,7-Dimethoxyquinazolin-4-ylamino)phenol hydrochloride (5a)

A mixture of compound **3** (120 mg, 0.53 mmol) and 3-amino-phenol (87 mg, 0.80 mmol) in 2-propanol afforded product **5a** as a light green solid (109 mg, 62%). ^1H NMR (300 MHz, $\text{DMSO}-d_6$) δ : 11.14 (1H, s, OH), 9.76 (1H, s, NH), 8.83 (1H, s, $-\text{N}=\text{CH}$), 8.21 (1H, s, aromatic-H), 7.32 (1H, s, aromatic-H), 7.26 (1H, d, $J = 8.1$ Hz, aromatic-H), 7.11–7.07 (2H, m, aromatic-H), 6.75 (1H, d, $J = 8.1$ Hz, aromatic-H), 4.02 (6H, s, $-\text{OCH}_3$). ESI-MS: m/z (332, MH^+).

4.1.4. 4-(6,7-Dimethoxyquinazolin-4-ylamino)phenol hydrochloride (5b)

Compound **3** (200 mg, 0.89 mmol) and 4-aminophenol (129 mg, 1.16 mmol) in 2-propanol gave product **5b** as a green solid (184 mg, 62%). ^1H NMR (300 MHz, $\text{DMSO}-d_6$) δ : 11.02 (1H, s, NH), 9.70 (1H, s, OH), 8.75 (1H, s, $-\text{N}=\text{CH}$), 8.13 (1H, s, aromatic-H), 7.40 (2H, d, $J = 8.7$ Hz, aromatic-H), 7.26 (1H, s, aromatic-H), 6.87 (2H, d, $J = 6.6$ Hz, aromatic-H), 3.99 (6H, s, $-\text{OCH}_3$). ESI-MS: m/z (298, MH^+).

4.1.5. (6,7-Dimethoxyquinazolin-4-yl)-(2-methoxyphenyl)-amine hydrochloride (5c)

Compound **3** (80 mg, 0.35 mmol) and 2-methoxyaniline (88 mg, 0.71 mmol) in 2-propanol gave product **5c** as a dark brown solid (64 mg, 53%). ^1H NMR (300 MHz, $\text{DMSO}-d_6$) δ : 11.06 (1H, s, NH), 8.71 (1H, s, $-\text{N}=\text{CH}$), 8.16 (1H, s, aromatic-H), 7.44–7.38 (2H, m, aromatic-H), 7.31 (1H, s, aromatic-H), 7.22 (1H, d, $J = 7.8$ Hz, aromatic-H), 7.07 (1H, t, $J = 7.5$ Hz, aromatic-H), 4.00 (3H, s, $-\text{OCH}_3$ of quinazoline), 3.98 (3H, s, $-\text{OCH}_3$ of quinazoline), 3.79 (3H, s, $-\text{OCH}_3$ of anisidine). ESI-MS: m/z (348, MH^+).

4.1.6. (6,7-Dimethoxyquinazolin-4-yl)-(4-methoxyphenyl)-amine hydrochloride (5d)

Compound **3** (120 mg, 0.53 mmol) and 4-methoxyaniline (131 mg, 1.06 mmol) in 2-propanol gave **5d** as a dark green solid (115 mg, 63%). ^1H NMR (300 MHz, $\text{DMSO}-d_6$) δ : 11.22 (1H, s, NH), 8.78 (1H, s, $-\text{N}=\text{CH}$), 8.21 (1H, s, aromatic-H), 7.55 (2H, d, $J = 6.9$ Hz, aromatic-H), 7.30 (1H, s, aromatic-H), 7.06 (2H, d, $J = 6.9$ Hz, aromatic-H), 4.00 (6H, s, $-\text{OCH}_3$ of quinazoline), 3.81 (3H, s, $-\text{OCH}_3$ of anisidine). ESI-MS: m/z (346, MH^+).

4.1.7. (6,7-Dimethoxyquinazolin-4-yl)-*o*-tolylamine hydrochloride (5e)

Compound **3** (90 mg, 0.40 mmol) and 2-methylaniline (52 mg, 0.48 mmol) in 2-propanol gave product **5e** as a white solid (70 mg, 53%). ^1H NMR (300 MHz, $\text{DMSO}-d_6$) δ : 11.28 (1H, s, NH), 8.71 (1H, s, $-\text{N}=\text{CH}$), 8.21 (1H, s, aromatic-H), 7.42–7.39 (1H, m, aromatic-H), 7.36–7.33 (3H, m, aromatic-H), 7.31 (1H, s,

aromatic-H), 4.00 (3H, s, –OCH₃), 3.99 (3H, s, –OCH₃), 2.21 (3H, s, –CH₃). ESI-MS: *m/z* (330, MH⁺).

4.1.8. (6,7-Dimethoxyquinazolin-4-yl)-*p*-tolylamine hydrochloride (5f)

Compound **3** (90 mg, 0.40 mmol) and 4-methylaniline (52 mg, 0.48 mmol) in 2-propanol gave product **5f** as a light green solid (80 mg, 60%). ¹H NMR (300 MHz, DMSO-*d*₆) δ: 11.23 (1H, s, NH), 8.79 (1H, s, –N=CH), 8.22 (1H, s, aromatic-H), 7.54 (2H, d, *J* = 8.4 Hz, aromatic-H), 7.31 (1H, s, aromatic-H), 7.30 (2H, d, *J* = 8.1 Hz, aromatic-H), 4.00 (3H, s, –OCH₃), 3.99 (3H, s, –OCH₃), 2.36 (3H, s, –CH₃). ESI-MS: *m/z* (330, MH⁺).

4.1.9. (2,3-Dichlorophenyl)-(6,7-dimethoxyquinazolin-4-yl)amine hydrochloride (5g)

Compound **3** (80 mg, 0.35 mmol) and 2,3-dichloroaniline (115 mg, 0.71 mmol) in 2-propanol gave product **5g** as a white solid (77 mg, 57%). ¹H NMR (300 MHz, DMSO-*d*₆) δ: 11.61 (1H, s, NH), 8.82 (1H, s, aromatic-H), 8.24 (1H, s, aromatic-H), 7.75 (1H, dd, *J* = 6.6, 2.4 Hz, aromatic-H), 7.71 (1H, s, aromatic-H), 7.56 (1H, dd, *J* = 8.4, 2.4 Hz, aromatic-H), 7.35 (1H, s, aromatic-H), 4.01 (3H, s, –OCH₃), 4.00 (3H, s, –OCH₃). ESI-MS: *m/z* (386, MH⁺).

4.1.10. 4-(6,7-Dimethoxyquinazolin-4-ylamino)benzonitrile hydrochloride (5h)

Compound **3** (80 mg, 0.35 mmol) and 4-cyanoaniline (86 mg, 0.71 mmol) in 2-propanol gave product **5h** as a white solid (79 mg, 66%). ¹H NMR (300 MHz, DMSO-*d*₆) δ: 11.21 (1H, s, NH), 8.90 (1H, s, –N=CH), 8.23 (1H, s, aromatic-H), 8.02 (2H, d, *J* = 8.4 Hz, aromatic-H), 7.95 (2H, d, *J* = 8.7 Hz, aromatic-H), 7.32 (1H, s, aromatic-H), 4.03 (3H, s, –OCH₃), 4.01 (3H, s, –OCH₃). ESI-MS: *m/z* (341, MH⁺).

4.1.11. 5-(6,7-Dimethoxyquinazolin-4-ylamino)-2-methylbenzonitrile hydrochloride (5i)

Compound **3** (80 mg, 0.35 mmol) and 3-cyano-4-methylaniline (97 mg, 0.71 mmol) in 2-propanol gave product **5i** as a white solid (86 mg, 69%). ¹H NMR (300 MHz, DMSO-*d*₆) δ: 11.28 (1H, s, NH), 8.88 (1H, s, –N=CH), 8.21 (1H, s, aromatic-H), 8.17 (1H, s, aromatic-H), 7.92 (1H, d, *J* = 8.4 Hz, aromatic-H), 7.59 (1H, d, *J* = 8.4 Hz, aromatic-H), 7.30 (1H, s, aromatic-H), 4.02 (3H, s, –OCH₃), 4.01 (3H, s, –OCH₃), 2.53 (3H, s, –CH₃). ESI-MS: *m/z* (357, MH⁺).

4.1.12. (4-Bromophenyl)-(6,7-dimethoxyquinazolin-4-yl)amine hydrochloride (5j)

Compound **3** (80 mg, 0.35 mmol) and 4-bromoaniline (48 mg, 0.43 mmol) in DMF afforded product **5j** as a white solid (70 mg, 57%). ¹H NMR (300 MHz, DMSO-*d*₆) δ: 11.19 (1H, s, NH), 8.83 (1H, s, –N=CH), 8.21 (1H, s, aromatic-H), 7.69 (4H, s, aromatic-H), 7.30 (1H, s, aromatic-H), 4.01 (3H, s, –OCH₃), 4.00 (3H, s, –OCH₃). ESI-MS: *m/z* (394, MH⁺).

4.1.13. (6,7-Dimethoxyquinazolin-4-yl)morpholin-4-ylamine hydrochloride (5k)

Compound **3** (100 mg, 0.44 mmol) and 1-aminomorpholine (92 mg, 0.89 mmol) in 2-propanol gave product **5k** as a yellow solid (42 mg, 29%). ¹H NMR (300 MHz, DMSO-*d*₆) δ: 8.41 (1H, s, –N=CH), 7.93 (1H, s, aromatic-H), 7.20 (1H, s, aromatic-H), 3.93 (6H, s, –2OCH₃), 3.79–3.76 (2H, m, N–CH₂–CH₂–), 3.70–3.66 (2H, m, N–CH₂–CH₂–), 2.99 (2H, m, O–CH₂–CH₂–), 2.90 (2H, m, O–CH₂–CH₂–). ESI-MS: *m/z* (327, MH⁺).

4.1.14. (6,7-Dimethoxyquinazolin-4-yl)-(4-methylpiperazin-1-yl)amine (5l)

Compound **3** (100 mg, 0.44 mmol) and 1-amino-4-methylpiperazine (79 mg, 0.67 mmol) in 2-propanol gave product **5l** as a yellow

solid (55 mg, 41%). ¹H NMR (300 MHz, DMSO-*d*₆) δ: 10.95 (1H, s, NH), 8.55 (1H, s, –N=CH), 8.04 (1H, s, aromatic-H), 7.32 (1H, s, aromatic-H), 3.97 (6H, s, –2OCH₃), 3.96–3.87 (6H, m, N–CH₂–CH₂–), 2.79 (3H, s, –CH₃), 2.78–2.73 (2H, m, N–CH₂–CH₂–). ESI-MS: *m/z* (304, MH⁺).

4.1.15. (6,7-Dimethoxyquinazolin-4-yl)-(2-morpholin-4-ylethyl)amine hydrochloride (5m)

Compound **3** (100 mg, 0.44 mmol) and 4-(2-aminoethyl)-morpholine (88 mg, 0.67 mmol) in 2-propanol gave product **5m** as a beige solid (114 mg, 73%). ¹H NMR (300 MHz, CDCl₃) δ: 8.56 (1H, s, –N=CH), 7.21 (1H, s, aromatic-H), 6.92 (1H, s, aromatic-H), 4.02 (3H, s, –OCH₃), 4.01 (3H, s, –OCH₃), 3.76 (4H, t, *J* = 4.5 Hz, O–CH₂–CH₂–), 3.71 (2H, t, *J* = 4.7 Hz, aliphatic-H), 2.76 (2H, t, *J* = 5.9 Hz, aliphatic-H), 2.59 (4H, t, *J* = 4.4 Hz, N–CH₂–CH₂–). ESI-MS: *m/z* (319, MH⁺).

4.1.16. (6,7-Dimethoxyquinazolin-4-yl)-(2-methoxyethyl)amine hydrochloride (5n)

Compound **3** (80 mg, 0.35 mmol) and 2-methoxyethylamine (54 mg, 0.71 mmol) in 2-propanol gave product **5n** as a brown solid (29 mg, 28%) after re-crystallization with 2-propanol. ¹H NMR (300 MHz, DMSO-*d*₆) δ: 9.73 (1H, s, NH), 8.75 (1H, s, –N=CH), 7.95 (1H, s, aromatic-H), 7.21 (1H, s, aromatic-H), 3.95 (3H, s, –OCH₃), 3.94 (3H, s, –OCH₃), 3.85 (2H, dd, *J* = 10.9, 5.2 Hz, aliphatic-H), 3.62 (2H, t, *J* = 5.4 Hz, aliphatic-H), 3.29 (3H, s, –CH₃). ESI-MS: *m/z* (264, MH⁺).

4.1.17. [2-(3,4-Dimethoxyphenyl)ethyl]-(6,7-dimethoxyquinazolin-4-yl)-amine Hydrochloride (5o)

Compound **3** (100 mg, 0.44 mmol) and 3,4-dimethoxyphenethylamine (125 mg, 0.67 mmol) in 2-propanol gave product **5o** as a brown solid (115 mg, 64%) after re-crystallization with 2-propanol. ¹H NMR (300 MHz, DMSO-*d*₆) δ: 8.36 (1H, s, –N=CH), 7.59 (1H, s, aromatic-H), 7.08 (1H, s, aromatic-H), 6.76 (3H, t, *J* = 7.9 Hz, aromatic-H), 3.89 (3H, s, –OCH₃), 3.87 (3H, s, –OCH₃), 3.74 (3H, s, –OCH₃), 3.72 (3H, s, –OCH₃), 2.94 (2H, t, *J* = 7.5 Hz, aliphatic-H), 2.74 (2H, t, *J* = 7.1 Hz, aliphatic-H). ESI-MS: *m/z* (406, MH⁺).

4.1.18. (6,7-Dimethoxyquinazolin-4-yl)naphthalen-1-ylamine hydrochloride (5p)

Compound **3** (80 mg, 0.35 mmol) and 1-aminonaphthalene (102 mg, 0.71 mmol) in 2-propanol gave product **5p** as a purple solid (92 mg, 71%). ¹H NMR (300 MHz, DMSO-*d*₆) δ: 11.62 (1H, s, NH), 8.66 (1H, s, –N=CH), 8.30 (1H, s, aromatic-H), 8.06 (2H, t, *J* = 6.9 Hz, aromatic-H), 7.89 (1H, d, *J* = 7.8 Hz, aromatic-H), 7.69–7.64 (2H, m, aromatic-H), 7.62–7.53 (2H, m, aromatic-H), 7.31 (1H, s, –OCH₃), 4.06 (6H, s, –2OCH₃). ESI-MS: *m/z* (368, MH⁺).

4.1.19. (4-Chlorobenzothiazol-2-yl)-(6,7-dimethoxyquinazolin-4-yl)amine hydrochloride (5q)

Compound **3** (80 mg, 0.35 mmol) and 2-amino-4-chlorobenzothiazole (102 mg, 0.71 mmol) in 2-propanol gave product **5q** as a green solid (16 mg, 9%) after re-crystallization with 2-propanol. ¹H NMR (300 MHz, DMSO-*d*₆) δ: 9.08 (1H, s, –N=CH), 8.35 (1H, s, aromatic-H), 8.03–7.98 (1H, m, aromatic-H), 7.57 (1H, d, *J* = 7.8 Hz, aromatic-H), 7.40 (1H, s, aromatic-H), 7.31–7.28 (1H, m, aromatic-H), 4.00 (6H, s, –2OCH₃). ESI-MS: *m/z* (409, MH⁺).

4.1.20. (6,7-Dimethoxyquinazolin-4-yl)pyridin-2-ylmethylamine (5r)

Compound **3** (100 mg, 0.44 mmol) and 2-aminomethylpyridine (243 mg, 2.22 mmol) in dioxane gave product **5r** as a beige solid (55 mg, 42%) through column purification. ¹H NMR (300 MHz, DMSO-*d*₆) δ: 8.63 (1H, d, *J* = 4.6 Hz, –N=CH–CH₂–), 8.59 (1H, s, –N=CH–N), 7.72 (1H, t, *J* = 7.7 Hz, aromatic-H), 7.40 (1H, d,

$J = 7.8$ Hz, aromatic-H), 7.22 (1H, s, aromatic-H), 7.18 (1H, m, aromatic-H), 7.07 (1H, s, aromatic-H), 5.30 (3H, s, aliphatic-H and NH), 4.02 (6H, s, -2OCH_3). ESI-MS: m/z (297, MH^+).

4.2. JAK2 activity assay

For determination of *in vitro* Jak2 kinase activity, we used HTScan[®] Jak2 Kinase Assay Kit (Cell Signaling Technology), which contains recombinant wild-type JAK2. Analysis was performed according to the manufacturer's protocol. Briefly, the kinase reaction was set up in the total volume as follows: 60 mmol/L Hepes (pH 7.5), 5 mmol/L MgCl_2 , 5 mmol/L MnCl_2 , 3 $\mu\text{mol/L}$ Na_3VO_3 , 1.25 mmol/L DTT, 20 $\mu\text{mol/L}$ ATP (200 $\mu\text{mol/L}$ ATP for competition experiments), 1.5 $\mu\text{mol/L}$ substrate peptide (0.3 and 0.15 $\mu\text{mol/L}$ for substrate competition experiments), and 10 U kinase. Increasing doses of test sample were added to the reaction and incubated at 25 °C for 1 h. The reaction was stopped by adding 50 μL /well of 50 mmol/L EDTA (pH 8). Each reaction (25 μL) was transferred in triplicate to a 96-well streptavidin-coated plate (Perkin-Elmer Life Sciences); 75 μL distilled water/well was added to each well and the reaction was incubated at room temperature for 1 h. After washing with PBS/T, monoclonal anti-phosphotyrosine antibody (p-Tyr¹⁰⁰; Cell Signaling Technology) was added (1:1000 in PBS/T with 1% bovine serum albumin) and incubated at room temperature for 1 h. After repeated washing with PBS/T, anti-mouse IgG, horseradish peroxidase-linked antibody (Cell Signaling Technology) was added (1:500 in PBS/T with 1% bovine serum albumin) and incubated for 30 min at 37 °C. After subsequent washing, TMB substrate was added, incubated for 5 min at room temperature, and stopped with an equal volume of 1 mol/L HCl. Absorbance was measured using a standard ELISA reader at 450 nm.

4.3. Cell culture

SC-OV-3, HeLa, and HT-29 cells were purchased from Korean Cell Line Bank. These cells were cultured in RPMI-1640 medium with 2.0 g/L sodium bicarbonate plus 10% fetal bovine serum, 100 U/mL penicillin, and 100 $\mu\text{g/mL}$ of streptomycin. All cell lines were maintained in a humidified incubator with an atmosphere of 95% air and 5% CO_2 at 37 °C.

4.4. Cytotoxicity assay

Cytotoxicity was assessed by the MTT assay. Briefly, cells were seeded at 1×10^5 cells/mL in each well containing 100 μL of RPMI-1640 medium supplemented with 10% FBS in a 96-well plate. After 24 h, various concentrations of tested samples were added. After 48 h, 50 μL of MTT (5 mg/mL stock solution, in PBS) were added per well and the plates were incubated for an additional 4 h. The medium was discarded and the formazan blue formed in the cells was dissolved with 100 μL of DMSO. The optical density was measured using a standard ELISA reader at 540 nm.

4.5. Protein extraction and Western blotting

After treatment with tested samples, cells growing on 10-cm dishes were lysed in 300 μL of ice-cold lysis buffer (20 mM Hepes at pH 7.4, 1 μM DTT, 20 μM EGTA, 10% glycerol, 50 μM glycerophosphate, 10 μM NaF, 1% Triton X-100, 1 mM PMSF, 1 mM Na_3VO_4 , 2 μM aprotinin, 100 μM leupeptin, 2 μM pepstatin, and 0.5 μM okadaic acid) on ice. The cell lysate was centrifuged at 14,000g for 15 min, and the supernatant fraction was collected for immunoblot. Equal amounts of protein (30–40 μg /well) were loaded and separated by SDS-PAGE (8–12%) and then electroblotted onto hybond-PVDF membranes (GE Healthcare Bio-Sciences Corp., NJ, USA). Membranes were blocked with 5% skim milk and

then sequentially incubated with the primary antibody overnight at 4 °C and secondary antibodies for 1 h at room temperature. Blots were processed for visualization using an enhanced chemiluminescence system (Pierce Biotechnology Inc., Rockford, IL, USA) and exposed to Kodak XAR-5 film (Rochester, NY, USA) to obtain the fluorographic images.

4.6. Luciferase assay

HT-29 cells were transfected with STAT3-dependent luciferase reporter construct pSTAT3-Luc plasmid together with phRL-TK using Lipofectamine LTX reagent (Invitrogen, Carlsbad, CA, USA) according to the manufacturer's protocols. Luciferase activity in cell lysates was determined by a dual luciferase reporter assay system (Promega, Madison, USA) and normalized to the Renilla luciferase activity of co-transfected phRL-TK. After 24 h, cells were serum-starved overnight and then treated with the test sample for 1 h. Cell extracts were prepared and assayed according to the manufacturer's protocols (Dual Luciferase Assay System; Promega).

4.7. RT-PCR

Total cellular RNA was isolated using Easy Blue[®] Kits (Intron Biotechnology, Seoul, Korea) according to the manufacturer's protocols. From each sample, 1 μg of RNA was reverse-transcribed (RT) using MuLV reverse transcriptase, 1 mM dNTP, and oligo(dT_{12–18}) 0.5 $\mu\text{g}/\mu\text{L}$. Then PCR analyses were performed on the aliquots of the cDNA preparations to detect c-myc, Bcl-xL and GAPDH (as an internal standard) gene expression using a thermal cycler (Perkin-Elmer Cetus, Foster City, CA, USA). The reactions were carried out in a volume of 25 μL containing 1 U of Taq DNA polymerase, 0.2 mM dNTP, 10 \times reaction buffer, and 100 pmol of 5' and 3' primers. After initial denaturation for 2 min at 94 °C, 30 amplification cycles were performed for c-myc (20 s of 94 °C denaturation, 10 s of 61 °C annealing, and 20 s of 72 °C extension), Bcl-xL (20 s of 94 °C denaturation, 30 s of 53 °C annealing, and 30 s of 72 °C extension) and GAPDH (60 s of 94 °C denaturation, 60 s of 61 °C annealing, and 120 s of 72 °C extension). The PCR primers used in this study are listed below and were purchased from Bioneer (Seoul, Korea): sense strand c-myc, 5'-GAT TCT CTG CTC TCCTCG ACG GAG-3', anti-sense strand c-myc, 5'-GCG CTG CGT AGT TGT GCT GAT GTG-3', sense strand Bcl-XL, 5'-CCC AGA AAG GAT ACA GCT GG-3', anti-sense strand Bcl-XL, 5'-GCG ATC CGA CTC ACC AAT AC-3', sense strand GAPDH, 5'-CCT GTT CGA CAG TCA CCG-3', anti-sense strand GAPDH, 5'-CGA CCA AAT CCG TTG ACT CC-3'. After amplification, portions of the PCRs were electrophoresed on 2% agarose gel and visualized by ethidium bromide staining and UV irradiation.

4.8. Flow cytometric detection

HT-29 cells were incubated until reaching 70–80% confluence. After treatment with or without treated samples, cells were harvested and fixed in 70% ethanol for 1 h on ice. After washing with PBS, cells were labeled with propidium iodide (50 $\mu\text{g/mL}$) in the presence of RNase A (100 $\mu\text{g/mL}$) and incubated at room temperature in the dark for 30 min and analyzed using the fluorescence-activated cell sorting (FACS) cater-plus flow cytometry (Becton-Dickinson Co., Heidelberg, Germany).

Acknowledgment

This work was supported by Korea Research Foundation Grant (KRF-2007-314-H00006).

References and notes

- (a) Zhou, Y. J.; Chen, M.; Cusack, N. A.; Kimmel, L. H.; Magnuson, K. S.; Boyd, J. G.; Lin, W.; Roberts, J. L.; Lengi, A.; Buckley, R. H.; Geahlen, R. L.; Candotti, F.; Gadina, M.; Changelian, P. S.; O'Shea, J. J. *Mol. Cell* **2001**, *8*, 959; (b) Kisseleva, T.; Bhattacharya, S.; Braunstein, J.; Schindler, C. W. *Gene* **2002**, *285*, 1; (c) Funakoshi-Tago, M.; Pelletier, S.; Matsuda, T.; Parganas, E.; Ihle, J. N. *EMBO J.* **2006**, *25*, 4763.
- (a) Yamaoka, K.; Saharinen, P.; Pesu, M.; Holt, V. E., 3rd; Silvennoinen, O.; O'Shea, J. J. *Genome Biol.* **2004**, *5*, 253; (b) Sayyah, J.; Sayeski, P. P. *Curr. Oncol. Rep.* **2009**, *11*, 117.
- Ihle, J. N.; Gilliland, D. G. *Curr. Opin. Genet. Dev.* **2007**, *17*, 8.
- Feng, J.; Witthuhn, B. A.; Matsuda, T.; Kohlhuber, F.; Kerr, I. M.; Ihle, J. N. *Mol. Cell. Biol.* **1997**, *17*, 2497.
- Saharinen, P.; Vihinen, M.; Silvennoinen, O. *Mol. Biol. Cell* **2003**, *14*, 1448.
- Luo, H.; Hanratty, W. P.; Dearolf, C. R. *EMBO J.* **1995**, *14*, 1412.
- (a) Levine, R. L.; Wadleigh, M.; Cools, J.; Ebert, B. L.; Wernig, G.; Huntly, B. J.; Boggon, T. J.; Wlodarska, I.; Clark, J. J.; Moore, S.; Adelsperger, J.; Koo, S.; Lee, J. C.; Gabriel, S.; Mercher, T.; D'Andrea, A.; Frohling, S.; Dohner, K.; Marynen, P.; Vandenberghe, P.; Mesa, R. A.; Tefferi, A.; Griffin, J. D.; Eck, M. J.; Sellers, W. R.; Meyerson, M.; Golub, T. R.; Lee, S. J.; Gilliland, D. G. *Cancer Cell* **2005**, *7*, 387; (b) James, C.; Ugo, V.; Le Couedic, J. P.; Staerk, J.; Delhommeau, F.; Lacout, C.; Garcon, L.; Raslova, H.; Berger, R.; Bennaceur-Griscelli, A.; Villeval, J. L.; Constantinescu, S. N.; Casadevall, N.; Vainchenker, W. *Nature* **2005**, *434*, 1144; (c) Baxter, E. J.; Scott, L. M.; Campbell, P. J.; East, C.; Fourouclas, N.; Swanton, S.; Vassiliou, G. S.; Bench, A. J.; Boyd, E. M.; Curtin, N.; Scott, M. A.; Erber, W. N.; Green, A. R. *Lancet* **2005**, *365*, 1054; (d) Kralovics, R.; Passamonti, F.; Buser, A. S.; Teo, S. S.; Tiedt, R.; Passweg, J. R.; Tichelli, A.; Cazzola, M.; Skoda, R. C. *N. Engl. J. Med.* **2005**, *352*, 1779; (e) Zhao, R.; Xing, S.; Li, Z.; Fu, X.; Li, Q.; Krantz, S. B.; Zhao, Z. J. *J. Biol. Chem.* **2005**, *280*, 22788; (f) Levine, R. L.; Belisle, C.; Wadleigh, M.; Zahrieh, D.; Lee, S.; Chagnon, P.; Gilliland, D. G.; Busque, L. *Blood* **2006**, *107*, 4139.
- (a) Lacronique, V.; Boureux, A.; Valle, V. D.; Poiriel, H.; Quang, C. T.; Mauchauffe, M.; Berthou, C.; Lessard, M.; Berger, R.; Ghysdael, J.; Bernard, O. A. *Science* **1997**, *278*, 1309; (b) Reiter, A.; Walz, C.; Watmore, A.; Schoch, C.; Blau, I.; Schlegelberger, B.; Berger, U.; Telford, N.; Aruliah, S.; Yin, J. A.; Vanstraelen, D.; Barker, H. F.; Taylor, P. C.; O'Driscoll, A.; Benedetti, F.; Rudolph, C.; Kolb, H. J.; Hochhaus, A.; Hehlmann, R.; Chase, A.; Cross, N. C. *Cancer Res.* **2005**, *65*, 2662; (c) Mercher, T.; Wernig, G.; Moore, S. A.; Levine, R. L.; Gu, T. L.; Frohling, S.; Cullen, D.; Polakiewicz, R. D.; Bernard, O. A.; Boggon, T. J.; Lee, B. H.; Gilliland, D. G. *Blood* **2006**, *108*, 2770.
- Meydan, N.; Grunberger, T.; Dadi, H.; Shahar, M.; Arpaia, E.; Lapidot, Z.; Leeder, J. S.; Freedman, M.; Cohen, A.; Gazit, A.; Levitzki, A.; Roifman, C. M. *Nature* **1996**, *379*, 645.
- (a) Ugo, V.; Marzac, C.; Teyssandier, I.; Larbret, F.; Lecluse, Y.; Debili, N.; Vainchenker, W.; Casadevall, N. *Exp. Hematol.* **2004**, *32*, 179; (b) Faderl, S.; Harris, D.; Van, Q.; Kantarjian, H. M.; Talpaz, M.; Estrov, Z. *Blood* **2003**, *102*, 630.
- Pissot-Soldermann, C.; Gerspacher, M.; Furet, P.; Gaul, C.; Holzer, P.; McCarthy, C.; Radimerski, T.; Regnier, C. H.; Baffert, F.; Drueckes, P.; Tavares, G. A.; Vangrevelinghe, E.; Blasco, F.; Ottaviani, G.; Ossola, F.; Scesa, J.; Reetz, J. *Bioorg. Med. Chem. Lett.* **2010**, *20*, 2609.
- (a) Wang, T.; Ledebuer, M. W.; Duffy, J. P.; Salituro, F. G.; Pierce, A. C.; Zuccola, H. J.; Block, E.; Shlyakter, D.; Hogan, J. K.; Bennani, Y. L. *Bioorg. Med. Chem. Lett.* **2010**, *20*, 153; (b) Wang, T.; Duffy, J. P.; Wang, J.; Halas, S.; Salituro, F. G.; Pierce, A. C.; Zuccola, H. J.; Black, J. R.; Hogan, J. K.; Jepson, S.; Shlyakter, D.; Mahajan, S.; Gu, Y.; Hoock, T.; Wood, M.; Furey, B. F.; Frantz, J. D.; Dauffenbach, L. M.; Germann, U. A.; Fan, B.; Namchuk, M.; Bennani, Y. L.; Ledebuer, M. W. *J. Med. Chem.* **2009**, *52*, 7938.
- Ledebuer, M. W.; Pierce, A. C.; Duffy, J. P.; Gao, H.; Messersmith, D.; Salituro, F. G.; Nanthakumar, S.; Come, J.; Zuccola, H. J.; Swenson, L.; Shlyakter, D.; Mahajan, S.; Hoock, T.; Fan, B.; Tsai, W. J.; Kolaczowski, E.; Carrier, S.; Hogan, J. K.; Zessis, R.; Pazhanisamy, S.; Bennani, Y. L. *Bioorg. Med. Chem. Lett.* **2009**, *19*, 6529.
- (a) Battle, T. E.; Frank, D. A. *Curr. Mol. Med.* **2002**, *2*, 381; (b) Yu, H.; Jove, R. *Nat. Rev. Cancer* **2004**, *4*, 97.
- Rane, S. G.; Reddy, E. P. *Oncogene* **2000**, *19*, 5662.
- (a) Darnell, J. E., Jr. *Science* **1997**, *277*, 1630; (b) Zamo, A.; Chiarle, R.; Piva, R.; Howes, J.; Fan, Y.; Chilosi, M.; Levy, D. E.; Inghirami, G. *Oncogene* **2002**, *21*, 1038.
- Amin, H. M.; McDonnell, T. J.; Ma, Y.; Lin, Q.; Fujio, Y.; Kunisada, K.; Leventaki, V.; Das, P.; Rassidakis, G. Z.; Cutler, C.; Medeiros, L. J.; Lai, R. *Oncogene* **2004**, *23*, 5426.